JOURNAL OF BIOMEDICAL OPTICS 3(3), 364–372 (JULY 1998)

SCATTERING OF LIGHT BY A RED BLOOD CELL

A. G. Borovoi,[†] E. I. Naats,[†] and U. G. Oppel[‡]
[†]Institute of Atmospheric Optics, Russian Academy of Science, Tomsk, 634055, Russia; [‡]Ludwig Maximilian University, Institute of Mathematics, Munich, Germany

(Paper JBO-140 received Mar. 20, 1997; revised manuscript received Oct. 25, 1997; accepted for publication May 6, 1998.)

ABSTRACT

The optical parameters of a red blood cell suspended in the blood plasma and, namely, the scattering and absorption cross sections and the scattering phase function describing the small-angle distribution of the scattered light are calculated. Dependence of the optical parameters on all possible values of size, shapes, orientations, hemoglobin concentration, and oxygenation degree is considered. The data are calculated with the so-called straight-ray approximation. The accuracy of the approximation is estimated by comparison with the Mie theory. © *1998 Society of Photo-Optical Instrumentation Engineers.* [S1083-3668(98)01003-X]

Keywords erythrocyte; scattering; cross section; scattering phase function.

1 INTRODUCTION

The optical parameters of a red blood cell (RBC) and, namely, the scattering cross section σ_s, the absorption cross section σ_a, and the scattering phase function p describing the angular distribution of scattered light are of great interest for purposes of optical diagnostics of the blood and tissues.

The simplest method of measuring these optical parameters of a single cell is realized, for example, in flow cytometers[1,2] where only one particle travels across the illuminated volume during the measurement time. Here, the optical parameters of every cell may, in principle, be measured using any standard technique. The optical parameters themselves are not, of course, the final goal of various diagnostic methods. The full diagnostic information would be the RBC geometrical and physical parameters: size, shape, and the refractive index. The latter value is connected with concentration and oxygenation degree of hemoglobin inside RBC. So, optical measurements only give the initial data for retrieving the geometrical parameters and the refractive index.

The relation between the optical and geometrical parameters could be obtained either from analytical or numerical solution of the problem of light scattering by a single RBC. At the same time, it is well known that the problem of light scattering by one particle is cumbersome; it may be solved only numerically. Even in the simplest case of a homogeneous sphere, a solution to this problem is an infinite series called the Mie theory series.[3] Few shapes like a spheroid allow one to write down the similar series. As a result, previous authors mainly had to ignore the nonsphericity of RBCs, dealing only with the Mie theory.

Fortunately, the blood cells have an important property: they are optically soft, i.e., the real part of their refractive index only slightly differs from that of the surrounding plasma

$$|\mathrm{Re}m-1|\ll 1. \tag{1}$$

The condition (1) makes it possible to obtain a solution of the scattering problem quite in a simple and physically obvious analytical form usually referred to as the anomalous diffraction approximation.[3] The simplicity of the equations obtained allows one to calculate optical parameters of a cell on a PC. In particular, we have developed a proper computer code called SASPASS (Small-Angle Scattering by Particles of Arbitrary Shape and Structure) for applications to the biomedical optics.

The purpose of this article is to obtain the optical parameters of RBCs suspended in the blood plasma taking into account the real parameters of RBCs: size, shape, orientation, and the refractive index.

It should be emphasized that the solution that is called, in this article, the straight-ray approximation, yields the simple relation between the optical and geometrical parameters of a particle. Therefore, this solution holds much promise for the development of methods for optical diagnostics of geometrical parameters of the blood cells.

It is worth noting here that the same problem of retrieving geometrical parameters of RBCs from the measured optical quantities is a necessary part of other optical methods. Thus, a standard technique is based on light scattering by an RBC ensemble forming a scattering medium. If the scattering me-

Address all correspondence to A. G. Borovoi. Fax: 3822-259086; E-mail: borovoi@acad.tomsk.su

dium is optically thin, one that can be made, for example, by diluting whole blood *in vitro*, the single scattering approximation is valid. In this case, any experimentally measured optical quantities are not quite the quantity of a single RBC but averaged over the ensemble. If a theoretical solution to the scattering problem for one RBC is known, one may invert the experimental data onto the RBC distributions over size, shape, etc., taking into account the ideas and methods developed in other fields of optics like optical particle sizing.[4]

The more complicated case is the scattering of light by an optically thick scattering medium like whole blood. Here, the process of multiple scattering strongly distorts the measured optical values and the relations between the optical quantities and the RBC parameters become more complex. In general, multiple scattering is described by the radiative transfer equation where the optical parameters of one particle are coefficients of this equation.[5] In biomedical optics, the radiative transfer equation is often used in the diffusion approximation where the coefficients turn to the truncated RBC optical parameters. For example, this approach is used in Refs. 5–7 for diagnostics of oxygen content in whole blood.

The RBC optical parameters obtained either theoretically or numerically are required for all the discussed methods. These necessary data are presented in this article.

2 STRAIGHT-RAY APPROXIMATION

Consider a plane electromagnetic wave,

$$\mathbf{E}_0(\mathbf{r}) = \mathbf{E}^0 \exp(ikz), \tag{2}$$

that is incident on a particle. Here $\mathbf{r}=(x,y,z)$ are the spatial coordinates, $k=2\pi/\lambda$, λ is the wavelength, and the particle will be described by the complex refractive index $m(\mathbf{r})$. If the particle is optically soft [Eq. (1)] and is much greater than the wavelength, as are a majority of biological cells for light radiation, the electromagnetic field inside the particle can be represented by the following equations:

$$\mathbf{E}(\mathbf{r}) = \mathbf{E}_0(\mathbf{r}) u(\mathbf{r}), \tag{3}$$

$$u(\boldsymbol{\rho},z) = \exp[i\Phi(\boldsymbol{\rho},z)], \tag{4}$$

$$\Phi(\boldsymbol{\rho},z) = k\int_{-\infty}^{z} [m(\boldsymbol{\rho},z')-1]dz'. \tag{5}$$

Here, one takes into account that the refraction of light rays by the particle is negligible, and therefore the influence of the particle on the traveling wave results in the complex-valued phase delay [Eq. (5)] along the longitudinal coordinate z. The lateral coordinates x and y are denoted as the two-dimensional variable $\boldsymbol{\rho}$. So, the large optically soft particle is equivalent to the proper amplitude-phase screen described by the function

$$\Phi(\boldsymbol{\rho}) = \Phi(\rho,\infty). \tag{6}$$

Equations (3)–(6) are true just behind the particle. Then the traveling wave becomes changed due to diffraction. At the distances $r \approx ka^2$ from the particle with the characteristic size a, the wave will undergo Fresnel diffraction from the screen [Eq. (6)]. In the wave zone $r \gg ka^2$, the wave is transformed due to the Fraunhofer diffraction into the superposition of the incident wave and the scattered wave, the latter being the diverging spherical wave concentrated, predominantly, within small scattering angles. The small angle scattering amplitude of the scattered wave is determined by the former amplitude-phase screen [Eq. (6)] according to the following two-dimensional Fourier transform:

$$f(\mathbf{n}) = \frac{k}{2\pi i}\int \exp(-ik\mathbf{n}\boldsymbol{\rho}) w(\boldsymbol{\rho}) d\boldsymbol{\rho}, \tag{7}$$

$$w(\rho) = [\exp(i\Phi(\boldsymbol{\rho}))-1] D(\boldsymbol{\rho}). \tag{8}$$

Here, $\mathbf{n}$ is the projection of the scattering direction on the plane $z=\text{const}$; $D(\boldsymbol{\rho})$ is the shadow function that is equal to unity inside the particle projection and is equal to zero outside. As the function [Eq. (7)] is essential under the small-angle condition $|\mathbf{n}| \ll 1$ only, it is convenient to expand formally the variable $\mathbf{n}$ over the whole plane.

It should be noted that if one neglects the first term of Eq. (8), the integral [Eq. (7)] turns to the Fraunhofer diffraction from a dark screen with the shape corresponding to the particle shadow. This case was called the normal diffraction by H. C. van de Hulst, while the case with the essential influence of the first term of Eq. (8) is called the anomalous diffraction.[3] So, Eqs. (3)–(8) are often referred to as the anomalous diffraction approximation.

The approximation (3)–(8) was used by a majority of authors in various fields of physics, too. It can be originated from either the geometrical optics or the wave parabolic equation. A number of names were proposed for this: eikonal approximation, WKB approximation, etc. It is preferable to call the approach (3)–(8) as the straight-ray approximation that reflects directly the essence of the approach.

Now it is easy to get the final equations for calculation of the RBC optical parameters. The cross sections of a particle are the following integrals over the shadow region behind the particle:

$$\sigma_s = \int |w(\boldsymbol{\rho})|^2 d\boldsymbol{\rho}, \tag{9}$$

$$\sigma_a = \int [1-|u(\boldsymbol{\rho})|^2] d\boldsymbol{\rho}, \tag{10}$$

$$\sigma = \sigma_s + \sigma_a = -2\,\mathrm{Re}\int w(\boldsymbol{\rho})d\boldsymbol{\rho}. \tag{11}$$

If energy of light is not absorbed inside a particle, we have $\sigma_a = 0$ and $\sigma_s = \sigma$.

The small-angle scattering phase function is described by the following two-dimensional Fourier transform:

$$p(\mathbf{n}) = |f(\mathbf{n})|^2/\sigma_s = \left(\frac{k}{2\pi}\right)^2 \int \exp(-ik\mathbf{n}\boldsymbol{\rho})S(\boldsymbol{\rho})d\boldsymbol{\rho}/S(0), \tag{12}$$

$$S(\boldsymbol{\rho}) = \int w(\boldsymbol{\rho}')w^*(\boldsymbol{\rho}'+\boldsymbol{\rho})d\boldsymbol{\rho}'. \tag{13}$$

It is seen that the function $w(\boldsymbol{\rho})$ having an evident geometrical sense determines both cross sections and the small-angle scattering patterns [Eq. (12)]. It should be emphasized that all geometrical and physical information contained in the optical parameters is restricted by the function $w(\boldsymbol{\rho})$. In its turn, the small-angle scattering pattern [Eq. (12)] bears the same information as the autocorrelation of the function $w(\boldsymbol{\rho})$ denoted as the S function [Eq. (13)].

In practice, the small-angle scattering patterns [Eq. (12)] are the ordinary data obtained experimentally. If one should use these experimental data for the inverse problems, i.e., for retrieval of some RBCs parameters, the usage of the S function has a number of advantages though the phase function and S function are equivalent mathematically.

Indeed, any measurements are always accompanied by some noise and errors. As is well known,[4] these experimentally observed errors are the main obstacle for solutions of the ill-posed inverse problems. So, the data processing that can suppress or filter out the errors becomes an important part for the retrieval algorithms.

In comparison with the phase function, the S function has a number of simple peculiar features that could be used as the filters matching the experimental data and the peculiarities. Namely, the S function differs from zero only in a domain of size of the particle diameter. At the point $\boldsymbol{\rho}=0$, the real part of the S function is maximum and its derivative has a jump while the imaginary part is equal to zero. Moreover, the equation

$$\mathrm{Im}\ S(\boldsymbol{\rho}) = 0 \tag{14}$$

is valid everywhere for two cases. In the first, a particle is symmetrical relative to a point $\boldsymbol{\rho}=0$:

$$w(\boldsymbol{\rho}) = w(-\boldsymbol{\rho}). \tag{15}$$

That is true for the majority of theoretical models of particles. In the second case, the function (8) is a real value that is true, for example, for absolutely absorbing particles.

The above mentioned features could be used to filter the experimental data. For this purpose, one has to transform the scattering pattern (12) into the S function and then to provide the manifestation of these obvious peculiarities. Therefore, the S functions are shown in parallel with the phase functions in this article.

3 GEOMETRICAL AND PHYSICAL PARAMETERS OF RBCS

A red blood cell can be assumed as an optically homogeneous particle with the shape described by the following function in the spherical coordinate system:

$$R(\theta,\varphi) = a\,\sin^q\theta + b. \tag{16}$$

Here $d = 2(a+b)$ is the diameter and $2b$ is the thickness in the center. As typical parameters for erythrocytes, we choose $d = 7.5\ \mu$m corresponding to $a = 3\ \mu$m and $b = 0.75\ \mu$m and the exponent q is estimated as $q = 5$ for best fitting with the standard shape. A reduction of the osmolarity of the suspending medium causes isovolumetric sphering of the cell. This evolution of the shape can be described by changing the parameters a, b, and q, where the case $q = 0$ corresponds to a sphere.

The ordinary parameter characterizing the RBCs for diagnostic purposes is the diameter d. It is known that the range of diameters for normal blood is from 5.7 to 9.35 μm with an average of 7.55 μm. A majority of erythrocytes (about 68%) are concentrated within the diameter interval from 7 to 8 μm. The mean diameter is an important diagnostic parameter. The shift of the average diameter to less than 7 μm or greater than 8 μm indicates some pathology.

The refractive index inside a RBC,

$$m = n + i\kappa, \tag{17}$$

depends on the optical wavelength in a complicated way. Figure 1 shows the complex refractive index versus the wavelength according to Refs. 5 and 8. Here, the real part is taken relative to the blood plasma with the refractive index of 1.35.

In addition, the refractive index [Eq. (17)] depends on the hemoglobin concentration, the concentration being varied for different persons. It is known that the value of the hemoglobin concentration c is in the intervals from 1.86 to 2.48 mmol/liter for women and from 2.02 to 2.71 mmol/liter for men. The linear dependence upon c is known[2]

$$n = n_0 + \alpha c, \tag{18}$$

$$\kappa = \beta c, \tag{19}$$

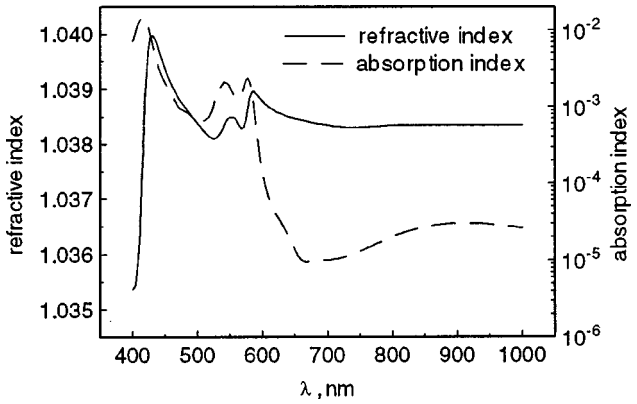

Fig. 1 Complex refractive index of a RBC as function of wavelengths. Oxygenation is 100%, the hemoglobin concentration is 2.036 mmol/liter. Following Ref. 8 in the range of 415–700 nm and Ref. 2 in the range of 700–1000 nm.

where α and β are constants depending on the wavelength and $n_0=1.35$ (Ref. 8) or $n_0=1.34$ (Ref. 2).

Besides, the imaginary part κ of the refractive index depends on the erythrocyte oxygenation especially in the wavelength range of 0.6–0.8 μm. According to Ref. 5 one has

$$\kappa=\kappa_h+\gamma(\kappa_0-\kappa_h), \tag{20}$$

where κ_h and κ_0 correspond to nonoxygenation and 100% oxygenation, respectively, and γ is the oxygenation degree; i.e., it is the part of the hemoglobin molecules oxygenated ($0\leqslant\gamma\leqslant1$).

4 SCATTERING AND ABSORPTION CROSS SECTIONS

As is known, the cross sections σ_s and σ_a of a RBC were calculated for the model of a homogeneous sphere only, i.e., within the framework of the Mie theory. In this section, these cross sections are calculated for the real shape of RBCs [Eq. (16)] using

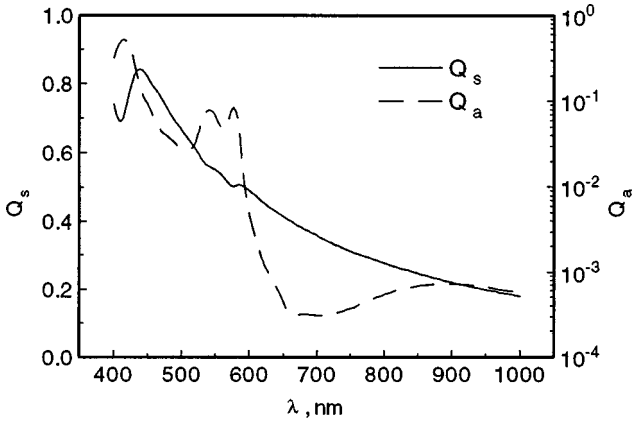

Fig. 2 Scattering and absorption efficiencies vs wavelengths. Normal incidence, $d=7.5$ μm.

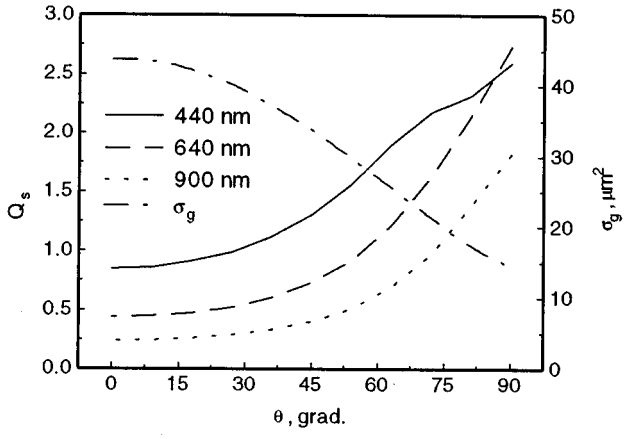

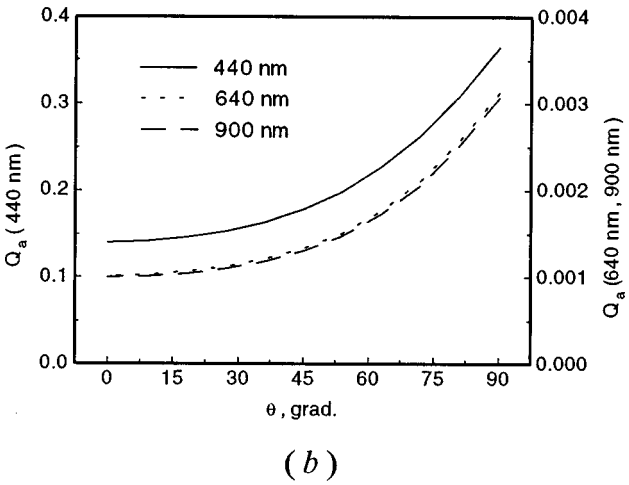

Fig. 3 Scattering (a) and absorption (b) efficiencies and the projection area σ_g vs RBC orientation, $d = 7.5$ μm.

Eqs. (9) and (10) of the straight-ray approximation. The accuracy of the approximation will be discussed later, in Sec. 6.

Instead of the absolute values of σ_s and σ_a, the dimensionless scattering and absorption efficiencies are more obvious:

$$Q_s=\sigma_s/\sigma_g, \quad Q_a=\sigma_a/\sigma_g, \tag{21}$$

where σ_g is the area of the RBC projection. For the normal incidence of light, the area is equal to the circle area $\pi d^2/4$ while the value σ_g is calculated numerically for the slant incidence that is presented in Figures 3(a) and 5(a).

The scattering and absorption cross sections depend on the following parameters: size, shape, orientation, complex refractive index, and wavelength of a light source. So, the efficiencies Q_s and Q_a are calculated as functions of one variable, the other parameters being fixed to the middle values.

Figure 2 shows the scattering and absorption efficiencies for all optical wavelengths according to the complex refractive index of RBC presented in

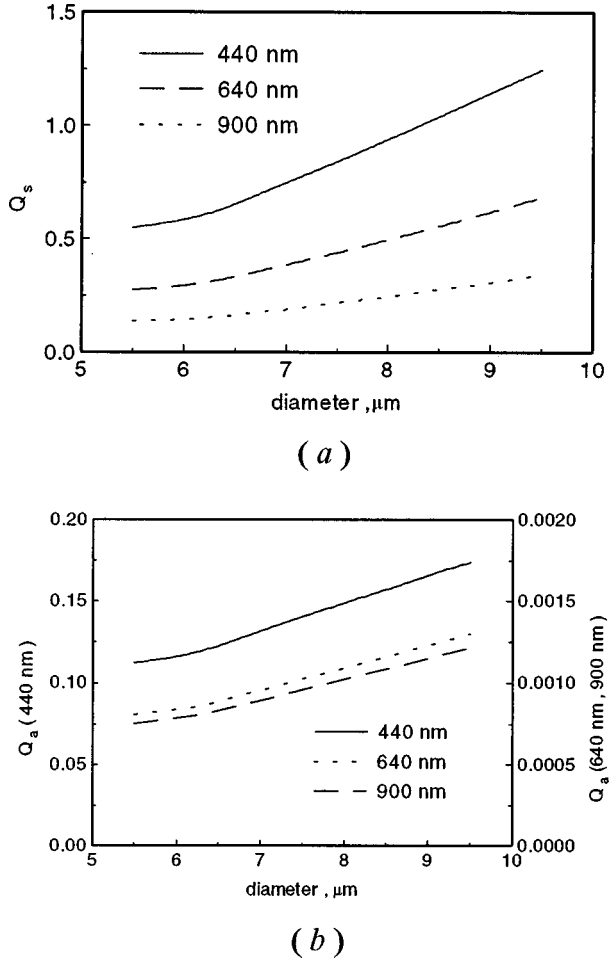

Fig. 4 Scattering (*a*) and absorption (*b*) efficiencies as function of RBC diameters, normal incidence.

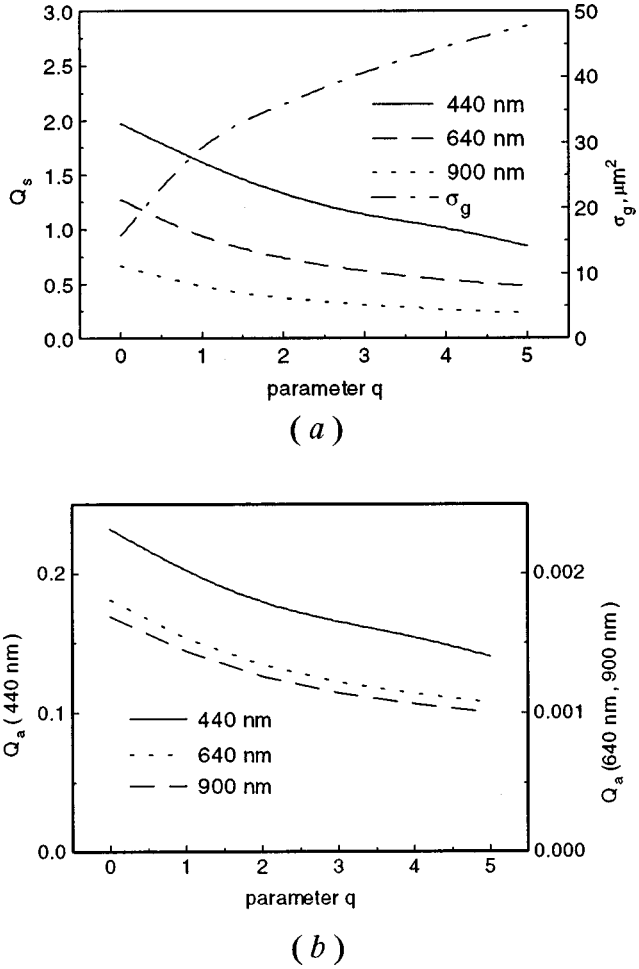

Fig. 5 Effect of RBC shape on the optical parameters. The RBC shape is transformed isovolumetrically. The normal erythrocyte shape corresponds to $q=5$ and $d = 7.5$ μm while $q=0$ corresponds to the sphere, normal incidence.

Figure 1. The essential dependence of the optical parameters on the wavelengths is clearly seen. Therefore, Figures 3–5 are calculated for three wavelengths chosen in different regions of the optical spectrum; the wavelengths are 440, 640, and 900 nm. These wavelengths are close to the wavelengths of the well known lasers: He–Cd laser (441 nm), He–Ne laser (632.8 nm), and a semiconductor laser (960 nm).

Figures 3(a) and 3(b) show the effect of RBC orientation on the efficiencies. The RBC orientation is determined by the tilt angle θ between the incident direction and the RBC symmetry axis. The normal incidence corresponds to $\theta=0$.

The dependence of the efficiencies on RBC size is presented in Figures 4(a) and 4(b). Here the diameter parameters a and b are varied proportionally.

It is known that the shape of an erythrocyte is varied isovolumetrically with reduction of the osmolarity of the suspending media. In our case, the shape was changed by the q parameter in Eq. (16). The parameters a and b were fitted numerically to provide the isovolumetric change of the shape. The obtained results are shown in Figure 5.

Figure 6 presents the results calculated for all possible hemoglobin concentrations within an erythrocyte. The calculations are carried out for 640 nm wavelength. The real and imaginary parts of the

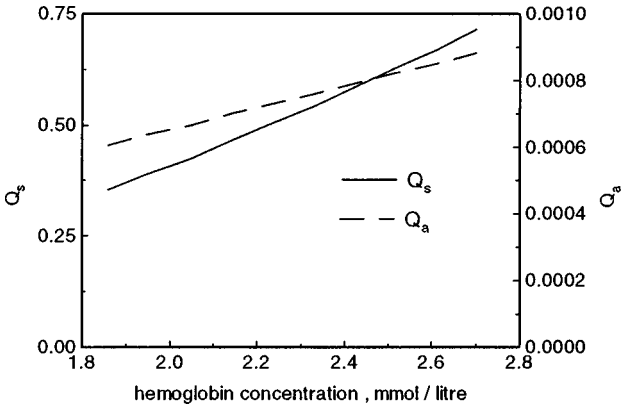

Fig. 6 Effect of the hemoglobin concentration on the optical parameters. The wavelength is 640 nm, normal incidence, d $=7.5$ μm.

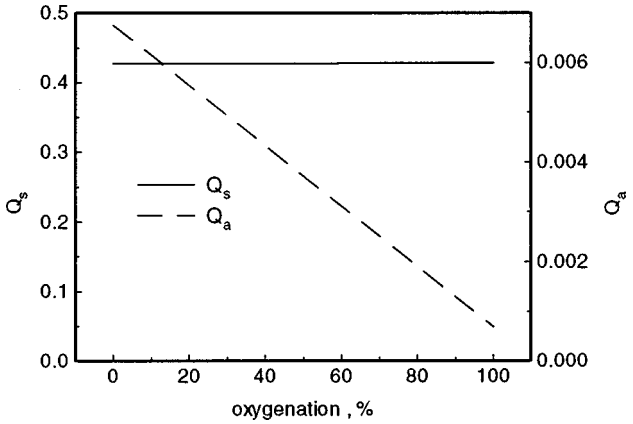

Fig. 7 Scattering and absorption efficiencies as function of the oxygenation degree. The wavelength is 640 nm, normal incidence, $d=7.5\ \mu$m.

refractive index are varied according to Eqs. (18) and (19). The magnitudes of the parameters α and β were determined from the data presented in Figure 1. For the wavelength of 640 nm, α is equal to 18.91 liter/mol and $\beta=0.009\,823$ liter/mol.

The degree of hemoglobin oxygenation has an effect on the imaginary part of the refractive index according to Eq. (20). For the wavelength of 640 nm, there is the following estimate for the ratio $\kappa_h/\kappa_0 \approx 10$.[5] Then, taking into account the data presented in Figure 1, one can get $\kappa_h=2\times10^{-4}$ and $\kappa_0=2\times10^{-5}$. In general, the degree of oxygenation can produce an effect on the real part of the complex refractive index, too. However, such data are unknown. Therefore, the real part was chosen as a constant for a fixed wavelength. Figure 7 shows the results calculated.

5 SMALL-ANGLE PHASE FUNCTIONS AND THE *S* FUNCTIONS

The phase function [Eq. (12)] is a standard optical value measured experimentally. In comparison with the integral parameters, σ_s and σ_a, the phase function has more detailed information on the geometrical and physical parameters of a scattering particle. In principle, the information may be retrieved from the experimental data and used for medical diagnostics.

In our case of the optically soft erythrocytes [Eq. (1)], the phase function is concentrated within the small scattering angles $\theta\cong\lambda/d$. On the one hand, it is rather difficult to measure the phase function with good accuracy in all scattering angles, due to this fact. On the other hand, the small-angle phase function bears the information on the geometrical and physical parameters of particles in a very simple and explicit form according to Eqs. (12) and (13), as compared to the Mie theory. Therefore, the inversion of the small-angle phase function for retrieval of the geometrical and physical parameters of erythrocytes is a much promising problem.

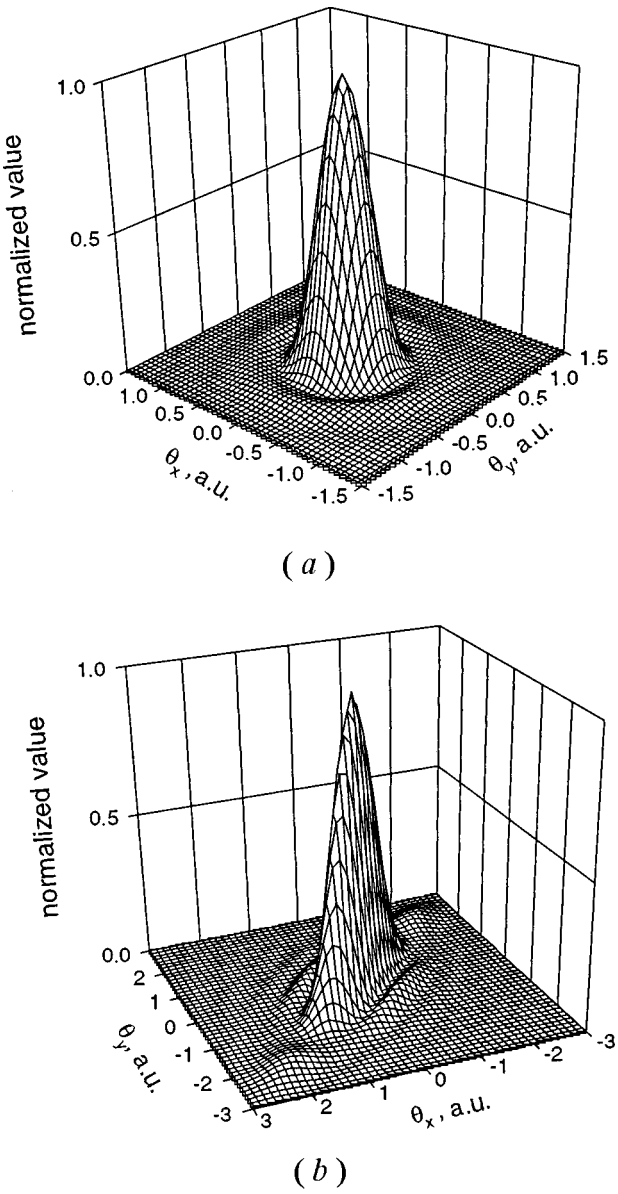

Fig. 8 Phase functions for various RBC orientations: (a) normal incidence $\theta=0$, (b) $\theta=\pi/2$ and $\varphi=\pi/4$. Wavelength is 440 nm, $d=7.5\ \mu$m.

In this section, the small angle scattering functions of erythrocytes are calculated within the straight-ray approximation. As it was discussed in Sec. 2, their two-dimensional Fourier transforms called the *S* functions are more advisable relative to the geometrical and physical parameters of erythrocytes. So, the *S* functions are calculated in parallel to the phase functions.

Figure 8(a) presents the phase function calculated for the normal orientation ($\theta=0$) and Figure 8(b) corresponds to the erythrocyte turned at $\theta=\pi/2$ and $\varphi=\pi/4$. It is seen that only the central and second maxima are essential. So, any retrieval of

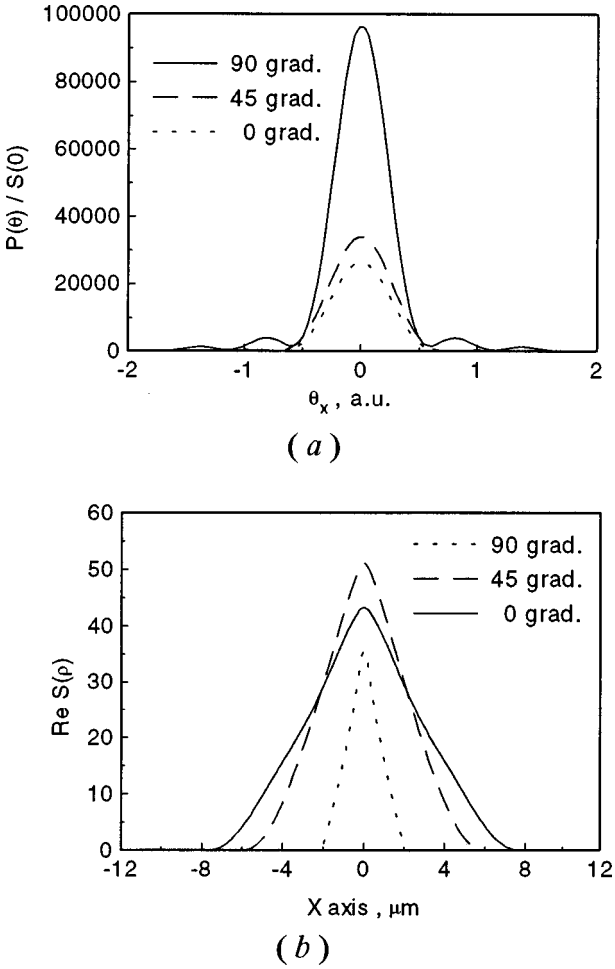

Fig. 9 Phase function (a) and the *S* function (b) for various RBC orientations. Rotation is around the *y* axis. Wavelength is 440 nm, $d=7.5$ μm.

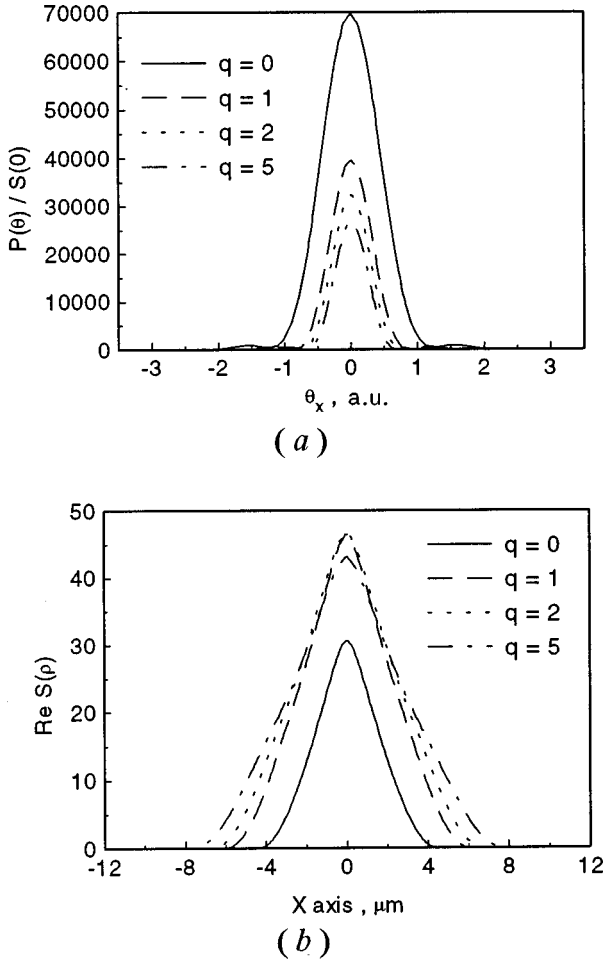

Fig. 10 Phase function (a) and the *S* function (b) for various isovolumetric shapes of RBC. Wavelength is 440 nm, $d=7.5$ μm, normal incidence.

information from the rapidly decreasing functions is difficult.

Figures 9(a) and 9(b) compare the phase functions and the *S* functions along the x axis ($y=0$) for various orientations of RBC. The RBC rotation is chosen around the y axis. Here, the imaginary part of the *S* function is equal to zero according to Eqs. (14) and (15). The analogous comparison is shown in Figures 10(a) and 10(b) for various isovolumetric shapes. It is seen that the *S* function is varied more dramatically with any change of the RBC geometrical parameters. Therefore, the *S* function is more sensitive as compared with the phase function.

The advantages of the *S* functions are most conspicuous for the erythrocytes with some irregular inclusions. In this case, the imaginary part of the *S* function is not equal to zero. As an illustration, a spherical inhomogeneity located at the distance of 2.75 μm from the center along the y axis has been considered below. The complex refractive index inside the sphere is taken to be three times greater than the RBC one. Figures 11(a), 11(b), and 11(c) show the phase function and the real and imaginary parts of the *S* function, respectively, for the sphere radius of 1 μm.

The inhomogeneity size is the main parameter that has an effect on these functions. Figures 12(a), 12(b), and 12(c) show the functions for various radii of the spherical inclusion. One can see that the imaginary part of the *S* function is the most sensitive to the inhomogeneity size.

6 COMPARISON WITH THE MIE THEORY

The accuracy of the straight-ray approximation for erythrocytes suspended in the blood plasma can be tested by comparison with the well-known Mie theory calculations that are applicable to spheres. For this purpose, the normal erythrocyte with the parameters described in Sec. 3 is transformed isovolumetrically into a sphere that gives the sphere diameter of 5.2 μm. The calculations of the scattering cross section versus optical wavelengths were carried out using three methods. The first method was the calculation according to the standard algorithm summarizing the Mie series. The refractive index of the sphere corresponded to the data in Fig-

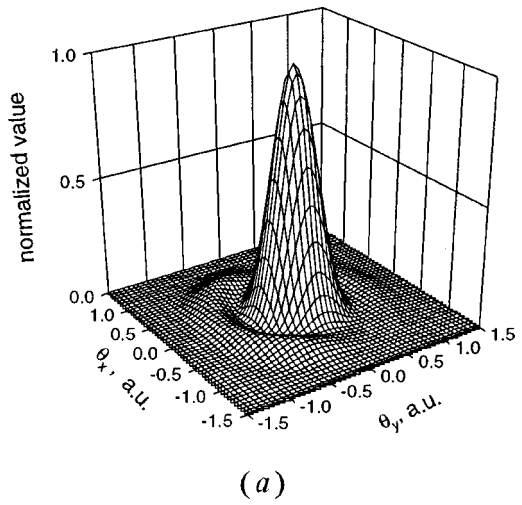

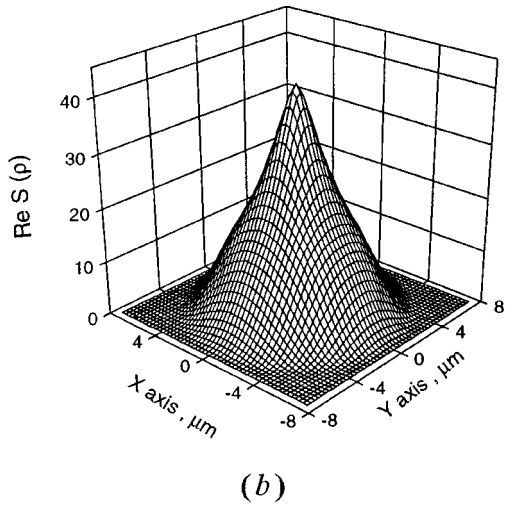

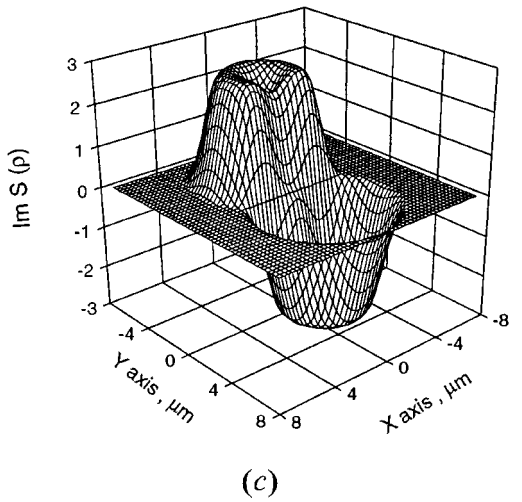

Fig. 11 Phase function (a), the real part (b), and the imaginary part (c) of the *S* function for RBC with a spherical inclusion. The center of the sphere is located at the distance of 2.75 μm from the RBC center along the *y* axis. The sphere radius is 1 μm. Wavelength is 440 nm, $d=7.5$ μm, normal incidence.

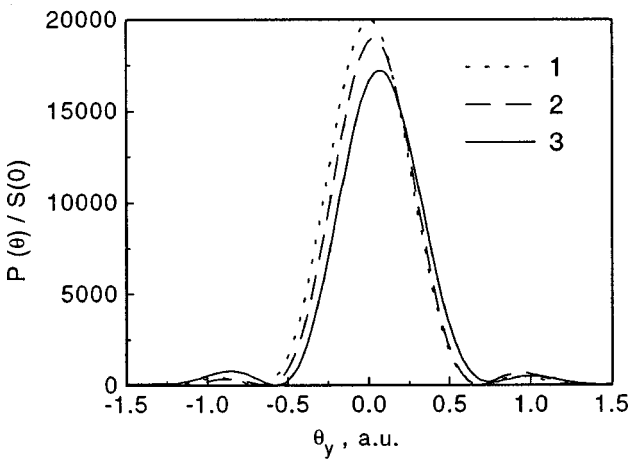

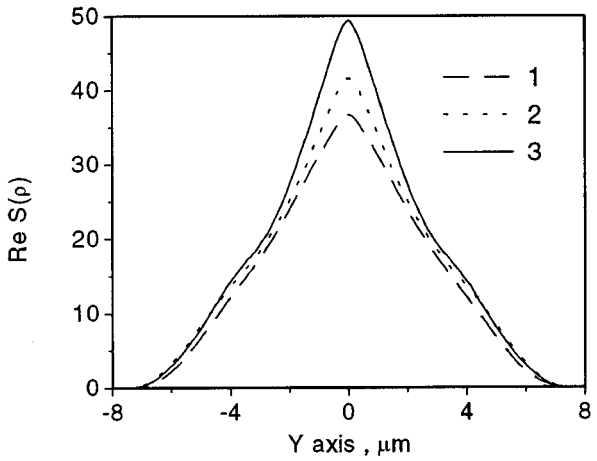

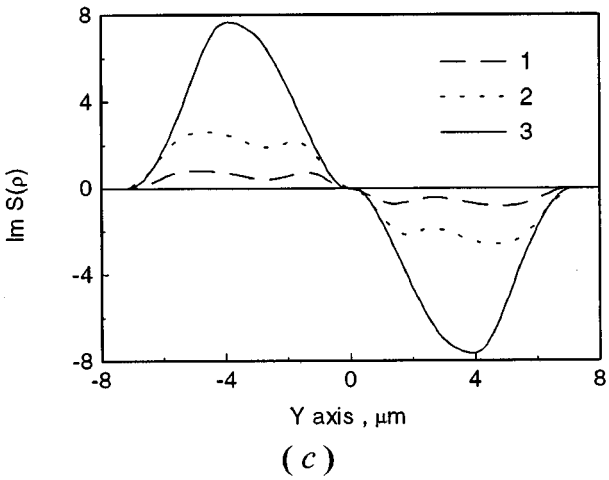

Fig. 12 Phase function (a), the real part (b), and the imaginary part (c) of the *S* function for RBC with a spherical inclusion vs the sphere radii: 1—$r=0.5$ μm, 2—$r=1$ μm, 3—$r=1.5$ μm. The center of the sphere is located at the distance of 2.75 μm (cases 1 and 2) and 2.0 μm (case 3) from the RBC center along the *y* axis. Wavelength is 440 nm, $d=7.5$ μm, normal incidence.

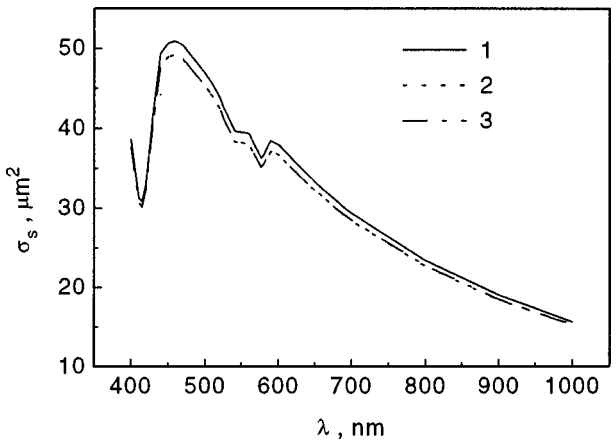

Fig. 13 Comparison between the Mie theory and the straight-ray approximation: (1) the Mie theory, (2) analytical, and (3) numerical calculation in the straight-ray approximation. Diameter of the sphere $d=5.2$ μm (isovolumetric transform for the normal RBC shape).

ure 1. The second method was the numerical calculation according to the analytical equation for the scattering cross section known for the homogeneous sphere in the straight-ray approximation.[5] The third method was the calculation using the SASPASS program. As a result, the data obtained with the last two methods were identical, as was verified with the given program. The difference between the scattering cross sections calculated with the Mie theory and with the straight-ray approximation did not exceed 4%, as is presented in Figure 13. It proves the accuracy of the data obtained above.

7 CONCLUSIONS

The first complete data concerning the effects of all the geometrical and physical parameters on the optical values of erythrocytes suspended in the blood plasma have been obtained. The real, nonspherical shape of erythrocytes is taken into consideration. As a result, the scattering and absorption cross sections and the phase function are calculated taking into account the geometrical and physical parameters, namely, size, shape, orientation, and the refractive index.

The calculations have been carried out in the so-called straight-ray approximation that is applicable to optically soft particles. The program SASPASS (Small-Angle Scattering by Particles of Arbitrary Shape and Structure) allows us to calculate the optical values of any optically soft particle with arbitrary orientations. The comparison with the Mie theory has shown the accuracy of the results obtained.

The two-dimensional Fourier transform of the small-angle phase function, called the *S* function, is proposed for diagnostics of the shape and structure of optically soft particles like erythrocytes instead of the phase function. The advantages of this approach are most conspicuous in the appearance of any irregular inclusions inside erythrocytes. In this case, the imaginary part of the *S* function becomes the most sensitive value.

REFERENCES

1. *Flow Cytometry and Sorting*, M. R. Melamed, T. Lindmo, and M. L. Mendelsohn, Eds., Wiley, New York (1990).
2. D. H. Tycko, M. H. Metz, E. A. Epstein, and A. Grinbaum, ''Flow-cytometric light scattering measurements of red blood cell volume and hemoglobin concentration,'' *Appl. Opt.* **24**(9), 1355–1365 (1985).
3. H. C. van de Hulst, *Light Scattering by Small Particles*, Wiley, New York (1957).
4. Feature issue on Optical Particle Sizing, *Appl. Opt.* **30**(33) (1991).
5. A. Ishimaru, *Wave Propagation and Scattering in Random Media*, Vols. 1,2, Academic, New York (1978).
6. V. Twersky, ''Absorption and multiple scattering by biological suspensions,'' *J. Opt. Soc. Am. A* **60**(8), 1084–1093 (1970).
7. D. R. Marble, D. H. Burns, and P. W. Cheung, ''Diffusion-based model of pulse oximetry: *in vitro* and *in vivo* comparison,'' *Appl. Opt.* **33**(7), 1279–1285 (1994).
8. M. Hammer (private communication).